

## Saturation transition in a monomer-monomer model of heterogeneous catalysis

This article has been downloaded from IOPscience. Please scroll down to see the full text article.

1990 J. Phys. A: Math. Gen. 23 4297

(<http://iopscience.iop.org/0305-4470/23/19/015>)

View [the table of contents for this issue](#), or go to the [journal homepage](#) for more

Download details:

IP Address: 129.252.86.83

The article was downloaded on 01/06/2010 at 08:59

Please note that [terms and conditions apply](#).

## Saturation transition in a monomer–monomer model of heterogeneous catalysis

D ben-Avraham†, D Considine‡, P Meakin§, S Redner‡ and H Takayasu‡

† Department of Physics, Clarkson University, Potsdam, NY 13676, USA

‡ Center for Polymer Studies and Department of Physics, Boston University, Boston, MA 02215, USA

§ Central Research and Development Department, E I duPont de Nemours and Co., Wilmington, DE 19880-0356, USA

Received 26 February 1990, in final form 24 May 1990

**Abstract.** We discuss the kinetics of an irreversible monomer–monomer model of heterogeneous catalysis. In this model, two reactive species,  $A$  and  $B$ , adsorb irreversibly onto single sites of a catalytic substrate; subsequently nearest-neighbour adsorbed  $AB$  pairs can bond to form a reaction product which desorbs from the substrate. The kinetics of this process is investigated in a mean-field approximation, where the catalytic substrate is considered to be an  $N$ -site complete graph. Two fundamental limits are identified: (a) the adsorption-controlled limit, where the reaction on the surface occurs quickly, so that the overall process is limited by the adsorption rate, and (b) the reaction-controlled limit, where adsorption occurs readily so that the overall reaction is limited by the conversion of unlike neighbouring monomers to an  $AB$  pair. By analysing the master equation for the probability density of coverage, we determine the rate at which the catalyst becomes ‘saturated’, i.e. completely covered by only one species. We show that the saturation time is proportional to  $N$ , and we also derive the probability distribution for the substrate coverage. Numerical simulations are performed on lattice substrates of finite spatial dimensionality  $d$  to test the range of validity of the mean-field approach. We find good agreement between simulations and mean-field theory for  $d = 2$  and  $3$ , but not for  $d = 1$ , suggesting that  $d = 2$  is a critical dimensionality for the monomer–monomer process.

### 1. Introduction

Catalysis is a fundamental kinetic process in which the rate of particular chemical reactions is enhanced by the presence of a catalyst. Heterogeneous catalysis involves more than one phase, with the reaction being enhanced near an interface. A typical example is oxidation of molecular species at a metal surface, a process which underlies the conversion of nitrous oxide to nitrogen dioxide in the presence of a platinum substrate in an automobile catalytic converter, for example. While oxidation does not readily occur in the gas phase, the reaction rate is greatly enhanced when the species are adsorbed on the substrate. After the adsorbates react on the catalyst, the product desorbs, thus allowing for the continuous operation of the system.

The classical approach for understanding the kinetics of heterogeneous catalysis is based upon Langmuir’s theory for adsorption, combined with rate equations for the subsequent reaction [1, 2]. Langmuir’s adsorption theory is based on all species being

adsorbed equivalently on the available lattice sites, with the subsequent reaction on the surface being described by the law of mass action. These are assumptions of a mean-field character, as microscopic details, such as local fluctuations in concentration and excluded volume interactions, are ignored. However, recent studies suggest that fluctuations are a crucial element in driving the kinetics [3–5]. For example, in the co-adsorption of CO and H<sub>2</sub> on Rh(111), a short-range repulsive interaction between the adsorbed H and CO molecules induces a segregation of the two species, under certain conditions [3]. Analogous segregation effects are observed in a number of related situations [4, 5]. This has a profound impact on the kinetics, because reactions between different adsorbed species can take place only along the boundaries in between the adsorbate islands.

An intriguing feature of the effect of fluctuations is the phenomenon of *saturation*, where the catalytic substrate ultimately becomes covered by one of the species only, thereby terminating the catalysis process. This has previously been referred to as ‘poisoning’ [6–12]. In the chemical literature, however, poisoning refers to a phenomenon whereby adsorption of a small amount of a foreign element destroys the catalytic character of a substrate [1]. Thus we adopt the term ‘saturation’ to denote the termination of a catalytic process when a single species completely covers the substrate. In this paper, we investigate the role of fluctuations in determining the kinetics of the saturation phenomenon for the monomer–monomer process. In this model [6–9], two different reactive substances, *A* and *B*, adsorb and stick to single sites of a catalytic substrate. Surface reactions are assumed to occur only between dissimilar species which are nearest-neighbours on the substrate. When the adsorption rates for the two species are different, the substrate quickly saturates with the preferred species. For equal adsorption probabilities, the substrate still saturates, but at a much slower rate and with equal probability of saturation by either of the two species. This latter saturation arises because of fluctuations in the number of reacting molecules and fluctuations in number space alone are sufficient to account for the kinetics of saturation.

These fluctuations are analysed in an approximation whereby the catalytic substrate is taken to be a *complete graph* [12], in which each of the *N* sites on the substrate are connected to each other. This description allows one to map the reaction onto a one-dimensional stochastic process, which we can then solve to obtain the reaction kinetics. Despite the approximations inherent in the complete graph formulation, our analytical results provide an attractive intuitive picture of the kinetics, and they agree with our Monte-Carlo simulation results when the dimensionality of the substrate,  $d \geq 2$ . Thus we infer that  $d = 2$  is a critical dimensionality for the process. Although many of our results are easily appreciated, the methodology outlined here is immediately applicable to more complex and realistic models, such as the monomer–dimer catalysis reaction [6]. Thus our approach can serve as a useful starting point for understanding some of the intriguing features in this process, such as the existence of kinetic phase transitions and of a reactive steady state.

It is important to distinguish two basic limiting cases of catalysis. When the reaction on the surface occurs quickly, the process is limited by the adsorption rate. This is the *adsorption-controlled limit*. On the other hand, when adsorption occurs readily, the overall reaction is limited by the conversion of unlike monomers to *AB* pairs. This latter case is the *reaction-controlled limit*. While reaction-controlled processes constitute the majority of industrial applications, there are important examples of adsorption-limited processes, most notably the synthesis of ammonia and methanol [1].

In many instances, the kinetics in the reaction-controlled and adsorption-controlled limits are different. For the monomer–monomer model, however, we find only quantitative differences between these two cases. Thus we focus only on the two limiting regimes, where a relatively simple treatment can be given, rather than treating the general case of arbitrary adsorption and reaction rates.

In section 2, we define the monomer–monomer model, and elucidate the nature of the reaction-controlled and the adsorption-controlled limit. We also present a formulation for the kinetics on a complete-graph substrate. In section 3, we solve the kinetics on the complete graph in the adsorption-controlled limit. From this solution, basic information about the rate of saturation is obtained. In section 4, we present the parallel results for the reaction-controlled limit. In section 5, numerical data from Monte-Carlo simulations of the monomer–monomer process for various substrate dimensionalities are given, and are compared with our mean-field results. We conclude in section 6.

## 2. The monomer–monomer model

In a typical surface catalytic reaction event, there are five basic stages [1] as illustrated in figure 1: (i) transport of reactants to the catalytic substrate, (ii) reactants close to the substrate adsorb, (iii) reaction on the substrate, (iv) reaction products desorb, and (v) reaction products are transported away from the surface. Steps (ii)–(iv) may be either irreversible or reversible, and we shall restrict ourselves to purely irreversible reactions. We also neglect the possibility that the adsorbates can diffuse on the substrate. In many instances, a constant external supply of reactants is maintained. Accordingly, steps (i) and (v) can be taken to occur infinitely quickly. Furthermore, steps (iii) and (iv) are not distinguishable in our modelling, and we therefore combine (iii) and (iv) into a single step of reaction and simultaneous desorption of the product.

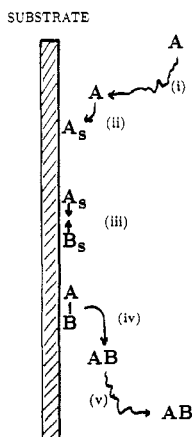


**Figure 1.** Schematic representation of the various stages of heterogeneous catalysis: (i) transport of reactants to the substrate, (ii) adsorption of reactants onto the substrate, (iii) surface reaction, (iv) desorption of products, (v) transport away from the substrate.

Under these restrictions, the reaction-limited process corresponds to the rate of adsorption (ii) being much larger than the rate of reaction (iii). Reactants adsorb readily but then reside on the substrate for a considerable time before any reaction occurs. Thus the surface reaction is the rate-limiting step of the catalysis. In the adsorption-limited process, the adsorption rate is much less than the reaction rate. Therefore many deposition attempts are needed before adsorption actually takes place. When reactive species happen to occupy neighbouring substrate sites, however, the catalytic reaction occurs immediately. Consequently, adsorption is the rate-limiting step of the overall process.

The realization of these steps in the monomer-monomer process involves first the adsorption of the two species,  $A$  and  $B$ , onto single substrate sites at respective rates  $k_A$  and  $k_B$ , to become the adsorbates,  $A_s$  and  $B_s$ . Secondly, when adsorbates of different species occupy nearest-neighbour substrate sites, they react at a rate  $k_r$ , to form a product which desorbs, thus leaving two sites available for repopulation by reactants. This process can be represented by



If  $k_A, k_B \gg k_r$ , the catalytic process is reaction-limited, while in the opposite case, the process is adsorption-limited.

In the adsorption-controlled limit, adsorption of an  $A$  (or a  $B$ ) is attempted onto an empty substrate site, with respective probabilities  $p = k_A/(k_A + k_B)$  and  $q = 1 - p$ . After adsorption, if there happens to be an  $A$  and a  $B$  which are nearest-neighbour (more than one such 'pair' could arise), then a reaction immediately occurs where one pair bonds and desorbs from the substrate. After these steps, the time is incremented by an amount appropriate for adsorption occurring at a constant rate. Repeating these steps yields a simple algorithm which models the kinetics in the adsorption-controlled limit.

In the reaction-controlled limit, the substrate quickly becomes full and it is convenient to start with a substrate that is randomly filled by equal amounts of  $A$ s and  $B$ s. For this case, the process consists of first choosing a pair of neighbouring lattice sites. If the two sites are occupied by the same species, no reaction is possible and an elemental reaction step has been completed. If the two sites are occupied by opposite species, a reaction occurs in which the reactants desorb, with each unoccupied site then being immediately refilled by either an  $A$  with probability  $p$ , or a  $B$  with probability  $q$ . The time is then incremented by  $1/N$ , and the reaction step begins anew.

To realize the mean-field limit, we model the substrate by an  $N$ -site complete graph with coordination number  $z = N - 1$ . On this graph, the spatial distribution of the reactants is irrelevant, and global densities suffice to describe the system. In the adsorption-controlled limit, the instantaneous reaction of  $AB$  pairs and the fact that all sites are reactively connected forbids the coexistence of  $A$ s and  $B$ s on the surface. The system can thus be characterized by the variable  $n = n_A - n_B$ , where  $n_A$  and  $n_B$  are the numbers of  $A$  and  $B$  adsorbates, respectively. The number difference  $n$  therefore equals  $n_A$  if the substrate contains only  $A$ s, and equals  $-n_B$  if the substrate contains only  $B$ s. If an  $A$  is deposited, either it adsorbs, or an  $AB$  pair is formed

which immediately desorbs. In either case,  $n$  is incremented by 1. Similarly, the attempted deposition of a  $B$  leads to a decrement of  $n$  by 1. Thus the number difference evolves according to a one-dimensional stochastic process on the interval  $-N, \dots, -1, 0, 1, \dots, N$ , with hopping probabilities which depend on  $p$  and on the number of vacant substrate sites (figure 2(a)). In the reaction-controlled limit, any sites that are cleared by a reaction are immediately refilled, and the lattice is always full. Consequently, one can characterize the state of the system by the single variable  $n = n_A - n_B = 2n_A - N$ , which changes by 0 or  $\pm 2$  in each elemental reaction event, and which ranges between  $-N$  and  $+N$  (figure 2(b)).

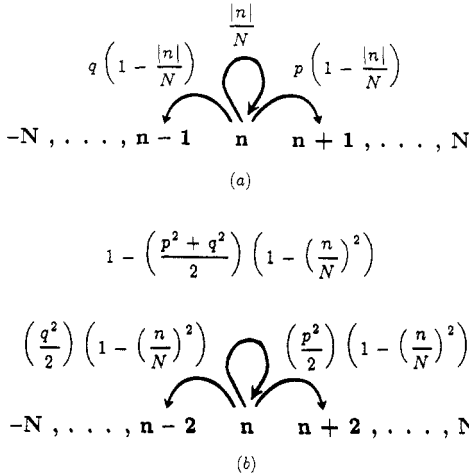


Figure 2. Schematic illustration of the stochastic process underlying the mean-field dynamics of the monomer–monomer model for (a) the adsorption-controlled limit, and (b) the reaction-controlled limit. The transition probabilities between the states are also shown.

In these one-dimensional stochastic processes, the saturated state is *absorbing*, as there is no transition possible which carries the system out of the saturated state. In a finite-size system, therefore, saturation must occur in a finite time, and the probability that the system has not yet saturated decreases exponentially in time, asymptotically [8, 12]. This saturation stems from the fluctuations due to the discreteness of a finite-size system when  $p = q$ . In the next sections, we solve for the kinetics of the monomer–monomer process on the complete graph and determine the nature of the saturation process.

### 3. Transient kinetics in the adsorption-limited process

On an  $N$ -site complete graph substrate, the hopping probabilities from state  $n$  to states  $n$  and  $n \pm 1$  in the stochastic process underlying the adsorption-limited case are

$$\begin{aligned}
 W(n \rightarrow n + 1) &= p(1 - |n|/N) \\
 W(n \rightarrow n - 1) &= q(1 - |n|/N) \\
 W(n \rightarrow n) &= |n|/N.
 \end{aligned}
 \tag{2}$$

If the surface becomes completely covered by a single species, i.e.  $n = \pm N$ , the hopping probabilities are identically zero, and this corresponds to the stopping of the reaction. If we define  $P_n(t)$  as the probability that the substrate has  $n$  adsorbed reactants at time  $t$ , then this probability obeys the master equation,

$$P_n(t + \Delta t) - P_n(t) = p \left( 1 - \frac{|n-1|}{N} \right) P_{n-1}(t) - \left( 1 - \frac{|n|}{N} \right) P_n(t) + q \left( 1 - \frac{|n+1|}{N} \right) P_{n+1}(t) \quad (3a)$$

for  $|n| \leq N - 1$ , while for  $|n| = N$ ,

$$\begin{aligned} P_N(t + \Delta t) - P_N(t) &= p \left( 1 - \frac{1}{N} \right) P_{N-1}(t) \\ P_{-N}(t + \Delta t) - P_{-N}(t) &= p \left( 1 - \frac{1}{N} \right) P_{-N+1}(t). \end{aligned} \quad (3b)$$

For a catalyst with a constant external supply of reactants, a time unit may be defined as the time required for an adsorption attempt onto each site of the substrate. Consequently, the time interval  $\Delta t$  for a single elemental event in the stochastic process is proportional to  $1/N$ . Henceforth, we take this proportionality constant to be unity.

Let us first examine the rate equation for the average surface concentration of reactants,  $x = \langle n \rangle / N$ ,

$$\dot{x} = (p - q)(1 - |x|). \quad (4)$$

For  $p \neq q$  the system approaches one of the absorbing states exponentially quickly, with a time constant  $\tau = 1/(p - q)$ , independent of the system size. When  $p = q$ , then  $\dot{x} = 0$ ; thus at the level of average densities, the system is static. Thus to find the approach to saturation requires analysis of the master equation.

The formal solution to the master equation can be derived by standard methods, see e.g. [13], from which basic facts about ultimate saturation can be extracted. However, the relative probabilities of saturation to all  $A$ s, or to all  $B$ s, can be found with no detailed calculations [12]. In the underlying stochastic process, the first passage probability to  $+N$  ( $A$ -saturated), starting from an empty system, can be expressed as  $p^N f_N(pq)$ , where  $p^N$  is the probability of a single stochastic 'path' from 0 to  $N$ , and  $f_N(pq)$  denotes the probability of all possible closed loops which can occur during the first passage from 0 to  $N$ . Similarly, the first passage probability to  $-N$  is  $q^N f_N(pq)$ . That is, for each stochastic path which leads to saturation of the system with all  $A$ s, there is a mirror image path which leads to saturation of the system with all  $B$ s. Consequently, the probability of eventual saturation to all  $A$ s is

$$\mathcal{P}_A = \frac{p^N}{p^N + q^N}. \quad (5)$$

Because this argument depends only on the symmetry  $p \leftrightarrow q$  and  $A \leftrightarrow B$  of the monomer-monomer process, equation (5) holds, not only for complete graphs, but for all  $N$ -site lattices, regardless of the spatial dimensionality.

Instead of presenting the solution to the discrete master equations, it is simpler and intuitively more revealing to employ a continuum description. Writing  $x \equiv n/N$ , with

$x$  ranging between  $-1$  and  $+1$  in steps of  $1/N$ , and defining the continuous probability  $P(x, t) dx = (1/N)P_n(t)$  as  $N \rightarrow \infty$ , one thereby finds that the probability density satisfies the Fokker–Planck equation,

$$\dot{P}(x, t) = (q - p) \frac{\partial}{\partial x} (1 - |x|) P(x, t) + \frac{1}{2N} \frac{\partial^2}{\partial x^2} (1 - |x|) P(x, t). \quad (6)$$

Notice that the diffusion coefficient is state dependent,  $D(x) = (1 - |x|)$ , reflecting the probability of successful adsorption being proportional to the fraction of empty sites,  $1 - |x|$ . Since  $D(x) \rightarrow 0$  as  $x \rightarrow \pm 1$ , the appropriate boundary condition for the probability density is  $P(x = \pm 1, t) < \infty$ . The evolution of the surface concentration therefore can be viewed as the motion of a random walk moving in a medium that is increasingly ‘sticky’ near the extremities of the absorbing interval. If the walk strays all the way to the endpoints where  $D = 0$ , the walk becomes completely mired and does not escape.

The solution to the Fokker–Planck equation in the interesting case of  $p = q = \frac{1}{2}$  is straightforward. Exploiting the symmetry about  $x = 0$ , we consider the interval  $[0, 1]$ , with the additional boundary condition of no flux passing through  $x = 0$ . Writing the eigenfunction expansion,

$$P(x, t) = \sum_{\lambda} A_{\lambda} P_{\lambda}(x) \exp\left(-\frac{\lambda^2}{8N} t\right) \quad (7)$$

we obtain the differential equation,

$$\frac{d^2}{dx^2} (1 - x) P_{\lambda}(x) + \frac{\lambda^2}{4} P_{\lambda}(x) = 0. \quad (8)$$

The substitution  $Q_{\lambda}(z) = z P_{\lambda}(x)$ , where  $z = 1 - x$ , transforms equation (8) to

$$\frac{d^2}{dz^2} Q_{\lambda}(z) + \frac{\lambda^2}{4z} Q_{\lambda}(z) = 0. \quad (9)$$

Because  $P_{\lambda}(x = 1)$  is finite,  $Q_{\lambda}(z = 0) = 0$ . The boundary condition on  $Q_{\lambda}(z)$  for  $z = 1$  is found by integrating equation (9) across  $x = 0$ . This gives

$$\frac{d}{dx} P_{\lambda}(x)|_{x=0} - P_{\lambda}(x)|_{x=0} = 0 \quad (10)$$

which therefore requires  $dQ/dz|_{z=1} = 0$ .

The general solution to equation (9) can be written in terms of the Bessel and Neumann functions of order one,  $J_1$  and  $Y_1$ , respectively [14, p362, 9.1.50]

$$Q_{\lambda}(z) = A\sqrt{z} J_1(\lambda\sqrt{z}) + B\sqrt{z} Y_1(\lambda\sqrt{z}). \quad (11)$$

The boundary condition  $Q_{\lambda}(z = 0) = 0$  implies  $B = 0$ , while the boundary condition at  $z = 1$  fixes  $\lambda$  to be one of the zeros of the Bessel function of order 0:  $\lambda_n = j_{0,n}$ , where the index  $n$  denotes the  $n$ th zero of this Bessel function. Therefore the general solution for  $P(x, t)$  is

$$P(x, t) = \sum_{n=1}^{\infty} A_n \frac{J_1(j_{0,n}\sqrt{1-|x|})}{\sqrt{1-|x|}} \exp\left(-\frac{j_{0,n}^2}{8N} t\right) \quad (12)$$



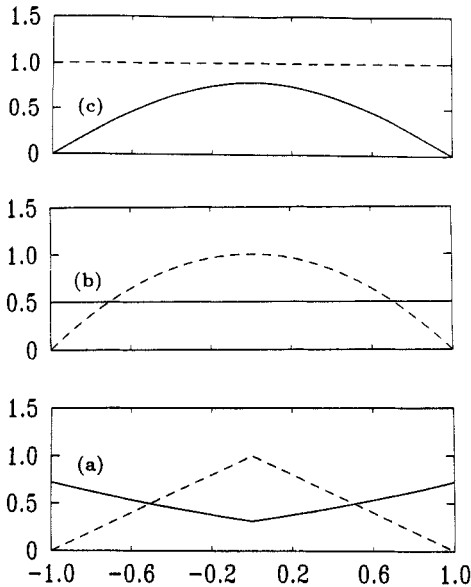


Figure 3. Plots of the lowest eigenmode of the probability distribution function,  $P(x, t)$ , against the density difference  $x$  for (a) the adsorption-controlled limit, (b) the reaction-controlled limit, and (c) a diffusive process on the same interval with a constant diffusion coefficient. The dependence of the corresponding diffusion coefficients versus  $x$  are shown dashed. The area under each of the curves has been normalized to 1.

where the  $A_n$  are fixed by initial conditions.

A plot of the lowest mode of this eigenfunction expansion is shown in figure 3(a). The probability density has a cusp at the origin, which arises from the discontinuous first derivative in  $D(x)$ , and the probability *increases* near the edges of the interval. This behaviour is opposite to that of constant diffusivity system, where the probability density asymptotically becomes one-half of a sine wave (figure 3(c)). Thus the qualitative effect of the state-dependent diffusion coefficient is to increase the probability of the system being close to the saturated state and also to inhibit the ultimate saturation, relative to a constant diffusivity system.

This intuition is confirmed by examining the survival probability,  $S(t) \equiv \int_{-1}^{+1} P(x, t) dx$ , i.e. the probability that the substrate has not saturated by time  $t$ . Integrating equation (12) over the interval  $(-1, 1)$ , it is clear that  $S(t)$  has the form

$$S(t) = \sum_n S_n \exp\left(-\frac{t}{\tau_n}\right) \quad (13)$$

where  $\tau_n = 8N/j_{0,n}^2$  is the characteristic decay time of the  $n$ th mode. The decay time of the longest-lived mode therefore is  $\tau_0 \approx 1.38N$ . For comparison, on an absorbing interval of the same length with a constant diffusivity  $D = 1$ , the corresponding decay time is  $\tau_0 = 4N/\pi^2 \approx 0.405N$ .

To find the mean time until saturation, we compute the mean first-passage time to reach either site  $N$  or site  $-N$  in the equivalent stochastic process. Let us denote this mean first-passage time as  $t_n$ , for a process which begins at site  $n$ , corresponding

to a substrate which initially contains  $n$  As. Then  $t_n$  obeys the recursion relation,

$$t_n = \frac{1}{2} \left(1 - \frac{n}{N}\right) (t_{n-1} + \Delta t) + \frac{1}{2} \left(1 - \frac{n}{N}\right) (t_{n+1} + \Delta t) + \frac{n}{N} (t_n + \Delta t) \quad (14)$$

which expresses the first-passage time from site  $n$  in terms of the first-passage times from neighbouring sites. Using  $\Delta t = 1/N$ , this recursion relation can be recast as

$$t_{n+1} + t_{n-1} - 2t_n = -\frac{2}{N-n}. \quad (15)$$

In the continuum limit this becomes

$$\frac{d^2 t(x)}{dx^2} = -\frac{2N}{1-x} \quad (16)$$

where  $t(x)$  now denotes the first-passage time to  $\pm 1$ , starting from an initial surface coverage  $x = n/N$ . Equation (16) must be supplemented with the boundary conditions  $t(1) = 0$  and  $dt/dx|_{x=0} = 0$ . Solving equation (16) yields

$$t(x) = 2N(1-x)(1 - \ln(1-x)). \quad (17)$$

It is interesting to compare this mean saturation time with the corresponding result for a constant diffusivity system. For such a case, the analogue of equation (16) is

$$\frac{d^2 t(x)}{dx^2} = -2N \quad (18)$$

when the time increment is  $\Delta t = 1/N$ , and the corresponding solution is

$$t(x) = N(1-x^2). \quad (19)$$

For  $x = 0$  the first-passage times for the two systems differ exactly by a factor of 2. However, for the initial condition  $x = 1 - 1/N$ , corresponding to a substrate with a single unoccupied site, the ratio of the saturation times for the two cases is proportional to  $\ln N$ . This slowing down stems from the inhibition of the adsorption process when the substrate is nearly filled.

#### 4. Transient kinetics in the reaction-limited process

In the reaction-limited process, whenever a catalytic reaction occurs, the two sites freed are immediately repopulated by either an  $A$  and a  $B$ , two  $A$ s, or two  $B$ s, with respective probabilities  $2pq$ ,  $p^2$ , and  $q^2$  [15]. In contrast to the adsorption-limited case,  $A$ s and  $B$ s can now co-exist on the substrate, subject only to the filling constraint,  $n_A + n_B = N$ . Since the substrate is always full, the probability that a reaction actually occurs is proportional to the product of the surface densities of  $A$ s and  $B$ s in the mean-field approximation. The hopping probabilities corresponding to these transitions in the underlying stochastic process are therefore

$$\begin{aligned} W(n_A, n_B \rightarrow n_A + 1, n_B - 1) &= 2p^2 \left(\frac{n_A}{N}\right) \left(1 - \frac{n_A}{N}\right) \\ W(n_A, n_B \rightarrow n_A - 1, n_B + 1) &= 2q^2 \left(\frac{n_A}{N}\right) \left(1 - \frac{n_A}{N}\right) \\ W(n_A, n_B \rightarrow n_A, n_B) &= 1 - 2(p^2 + q^2) \left(\frac{n_A}{N}\right) \left(1 - \frac{n_A}{N}\right). \end{aligned} \quad (20)$$

From these hopping probabilities, the rate equation for  $y$ , the average coverage of the substrate by  $A$ s is

$$\dot{y} = 2(p - q)y(1 - y). \tag{21}$$

For  $p \neq q$ , there is a net bias of either  $A$ s or  $B$ s, and the system saturates exponentially in time, with a characteristic decay time  $\tau = 1/(2(p - q))$ . For  $p = q = \frac{1}{2}$ , however, diffusive fluctuations drive the system to saturation. This dynamics can once again be investigated from the underlying master equation. Based on the hopping rates in equation (20), the master equations for  $p = q = \frac{1}{2}$  are

$$\begin{aligned} P_{n_A}(t + \Delta t) - P_{n_A}(t) &= \frac{1}{2} \left( \frac{n_A - 1}{N} \right) \left( 1 - \frac{n_A - 1}{N} \right) P_{n_A - 1}(t) \\ &\quad + \frac{1}{2} \left( \frac{n_A + 1}{N} \right) \left( 1 - \frac{n_A + 1}{N} \right) P_{n_A + 1}(t) - \left( \frac{n_A}{N} \right) \left( 1 - \frac{n_A}{N} \right) P_{n_A}(t) \end{aligned} \tag{22a}$$

for  $0 < n_A < N$ , while for  $n_A = 0, N$ , the master equations are

$$\begin{aligned} P_0(t + \Delta t) - P_0(t) &= \frac{1}{2} \left( \frac{1}{N} \right) \left( 1 - \frac{1}{N} \right) P_1(t) \\ P_N(t + \Delta t) - P_N(t) &= \frac{1}{2} \left( \frac{1}{N} \right) \left( 1 - \frac{1}{N} \right) P_{N - 1}(t). \end{aligned} \tag{22b}$$

In the continuum limit, we obtain the Fokker-Planck equation,

$$\dot{P}(y, t) = \frac{1}{2N} \frac{\partial^2}{\partial y^2} [y(1 - y) P(y, t)]. \tag{23}$$

It is convenient to transform to the density-difference variable  $x = 2y - 1$ , in order to compare directly with the Fokker-Planck equation for the adsorption-controlled case. One obtains

$$\dot{P}(x, t) = \frac{1}{2N} \frac{\partial^2}{\partial x^2} (1 - x^2) P(x, t). \tag{24}$$

Since the position dependence of the diffusion coefficient is qualitatively similar for both the adsorption-limited and reaction-limited processes, we expect qualitative similar dynamical behaviour in these two cases.

The eigenfunctions to the time-independent eigenvalue equation are the Gegenbauer polynomials [13, p 781, 22.6.5],  $C_n^\alpha(y)$ , with  $\alpha = 3/2$ . Thus the general solution to equation (24) is

$$P(x, t) = \sum_{n=0}^{\infty} A_n C_n^{3/2}(x) \exp \left[ \left( -\frac{n(n + 3) + 2}{2N} \right) t \right] \tag{25}$$

where the coefficients  $A_n$  are determined by the initial conditions. Amusingly, the lowest mode of this expansion is exactly a constant,  $C_0^{3/2}(x) = 1$ , which evidently arises

from the balance between the depletion of the probability density near the absorbing boundary and the inhibited diffusion as the endpoint is approached (figure 3(b)).

The mean saturation time, starting from a state containing  $n$  *As* obeys the recursion relation, in close analogy with equation (14),

$$t_n = \frac{1}{2} \left( \frac{n}{N} \right) \left( 1 - \frac{n}{N} \right) (t_{n-1} + t_{n+1}) + 1 - \left( \frac{n}{N} \right) \left( 1 - \frac{n}{N} \right) t_n + \Delta t. \quad (26)$$

Solving this equation in the continuum limit gives

$$t(x) = N \left[ (1-x) \ln \left( \frac{2}{1-x} \right) + (1+x) \ln \left( \frac{2}{1+x} \right) \right]. \quad (27)$$

To compare with corresponding results for the adsorption-controlled limit and also for a purely diffusive system, consider the ‘symmetric’ initial condition where  $x = 0$ , a lattice containing 50% *As* and 50% *Bs*. This is the analogue of the empty substrate initial condition in the adsorption-controlled limit. For  $x = 0$ , equation (27) gives  $t_0 = 2N \ln 2$ , compared with  $t_0 = 2N$  in the adsorption-controlled limit, and  $t_0 = N$  for pure diffusion. For the symmetric initial condition, saturation occurs faster in the reaction-controlled limit because the diffusion coefficient is always greater than that of the adsorption-controlled limit. On the other hand, for an initial condition of a single defect the saturation time is  $2 \ln N$ , asymptotically, for both cases.

## 5. Simulations

We now discuss our Monte-Carlo simulation results in both the reaction-controlled and the adsorption-controlled limits. For two- and three-dimensional substrates, the simulations are in close agreement with mean-field results. However, in one dimension, substantial disparities between simulations and mean-field theory occur. In particular, the mean saturation time is proportional to  $N^2$  for both the adsorption- and reaction-controlled limits, rather than being linear in  $N$ .

### 5.1. Adsorption-controlled limit

A direct simulation of the adsorption-controlled process is relatively inefficient, as there will be many attempts to adsorb a particle onto an already-occupied site before a successful adsorption finally occurs. This is especially true at late stages, when the substrate is nearly full. To overcome this difficulty, it is conventional to employ an algorithm in which particles are deposited only onto empty sites, and increment the time by  $1/N_e$ , where  $N_e = N - |n|$  is the number of empty lattice sites. Unfortunately, this simple construction is not, in principle, correct. For a fixed density of vacancies  $(1-x)$ , the time until the next successful adsorption is a fluctuating quantity, with only the average value equal to  $1/N_e$ . However, since the probability of successful adsorption after  $n$  deposition attempts is  $1 - (1-x)^{n+1}$ , one can still deposit particles onto empty lattice sites only, provided that each adsorption is accompanied by a time increase compatible with the above probability. This is achieved by picking a random number  $r$  evenly distributed in  $(0, 1)$  and assigning a time increment of  $[\ln(1-r)/\ln(1-x)]/N$ . With this method, no computer time is wasted on futile deposition attempts to occupied sites, and the physically correct time increment is employed.

It is instructive to compare the dynamics of these two algorithms. For the naive process of depositing particles on unoccupied sites and updating the time by  $1/N_e$ , the corresponding master equation for the complete graph is (compare with equation (3))

$$P_n(t + \delta t_n) - P_n(t) = pP_{n-1}(t) + P_n(t) + qP_{n+1}(t) \quad (28a)$$

for  $|n| \leq N - 1$ , while for  $|n| = N$ ,

$$\begin{aligned} P_n(t + \delta t_n) - P_n(t) &= pP_{n-1}(t) \\ P_{-n}(t + \delta t_n) - P_{-n}(t) &= pP_{-n+1}(t). \end{aligned} \quad (28b)$$

Here,  $\delta t_n = 1/N_e = 1/(N - |n|)$ . In the continuum limit, one obtains the Fokker-Planck equation

$$\dot{P}(x, t) = \frac{1}{2N} (1 - |x|) \frac{\partial^2}{\partial x^2} P(x, t) \quad (29)$$

which should be compared with equation (6). The two equations differ by a drift term, with a driving velocity that is of order  $1/N$ . This term is sometimes called the 'spurious flow', which is an example of the Itô-Stratonovich dilemma for the appropriate interpretation of the Fokker-Planck equation [16]. For the monomer-monomer model on the complete graph, we can prove that the first passage time to saturation is the same in the two interpretations. Owing to the smallness of the drift term, there were no significant differences in the numerical data for the probability distribution of coverage using the two algorithms. Nevertheless, it is useful to be cognisant of the shortcomings of the commonly accepted simulation method.

In figure 4, we plot the probability for the density difference on the substrate as a function of the density difference, in 1, 2 and 3 dimensions. The time has been chosen so that the saturation probability is  $\gtrsim 0.9$  for the three cases, so that the probability density should be dominated by the lowest eigenmode. In one dimension, the probability is peaked at zero density difference, while in two and three dimensions, the probability increases as the density difference tends to its limiting value of  $\pm 1$ . The behaviour in three dimensions is quantitatively very similar to that of mean-field theory (figure 3(a)). The size dependence of the mean saturation time,  $t_0$ , starting from an initially empty substrate is plotted in figure 5. In two and three dimensions the data suggest that  $t_0$  is roughly proportional to  $N$ . A linear regression analysis yields  $t_0 \sim 1.46N^{1.07}$  in two dimensions and  $t_0 \sim 1.83N^{1.02}$  in three dimensions, where these numerical values are accurate to within 10%. These compare reasonably well with  $t_0 = 2N$ , the mean-field result from equation (17). The slightly larger exponent value in two dimensions may be suggestive of a logarithmic correction in the saturation time.

On the other hand, the data for one dimension suggests that  $t_0 \simeq 0.11N^2$ . This quadratic dependence of the mean saturation time on  $N$  can be understood simply by considering the spatial arrangement of reactants in one dimension [9]. The system rapidly forms domains of *A* and *B* particles as the substrate fills, and the essential mechanism for saturation is the diffusion of all domain walls to the boundary of the system. On this basis, it is straightforward to show that the mean poisoning time grows as  $N^2$ .

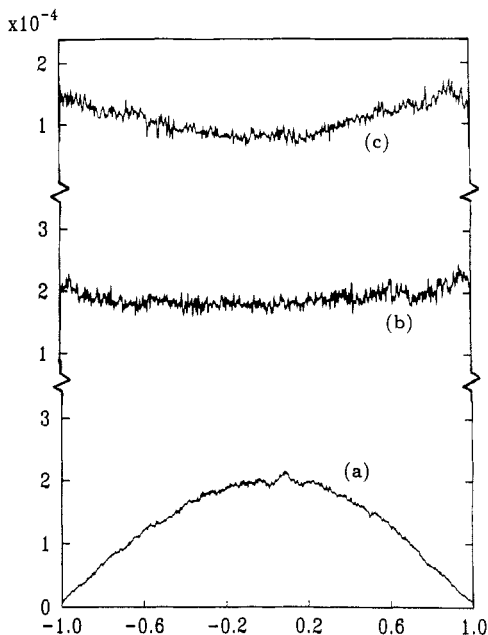


**Figure 4.** Simulation data for the probability distribution,  $P(x, t)$ , that the substrate is characterized by a density difference equal to  $x$  in the adsorption-controlled limit. (a) Results from averaging of 10 000 configurations of a one-dimensional substrate of linear dimension 250 for times  $16\,000 \leq t \leq 20\,000$ . (b) 5000 configurations for a square of 256 sites with  $1000 \leq t \leq 1500$ . (c) 9000 configurations for a cube of 216 sites with  $1000 \leq t \leq 1200$ .

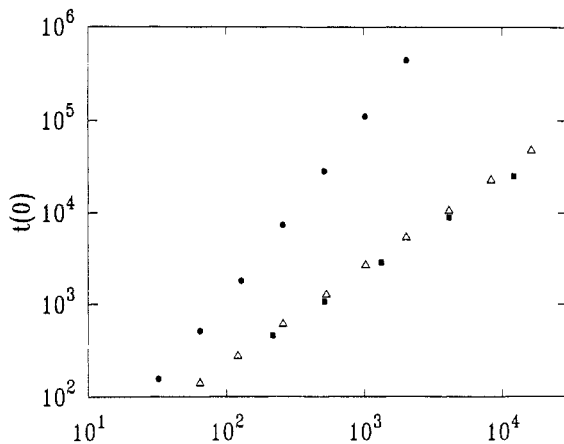


**Figure 5.** Dependence of the mean saturation time on the number of sites for an initially empty system, in the adsorption-controlled limit. ●, one dimension; Δ, two dimensions; and ■, three dimensions.

### 5.2. Reaction-controlled limit

For convenience in implementing a numerical algorithm, we choose the initial configuration to be a completely full lattice, with half of the sites randomly occupied

by each species. The simulation results for  $P(x, t)$  for one and two dimensions are depicted in figure 6. The relatively flat probability density in two dimensions is quite similar to the mean-field picture, while the probability density in one dimension is peaked. Similarly, the mean saturation time appears to grow as  $1.22N^{1.1}$  in two dimensions, compared with the mean-field prediction of  $t_0 = (2 \ln 2)N \approx 1.38N$ , while  $t_0 \sim 0.07N^{2.07}$  in one dimension (figure 7). Once again, there appears a qualitative change when the substrate dimensionality is one, which is analogous to the pattern of behaviour in the adsorption-controlled limit.

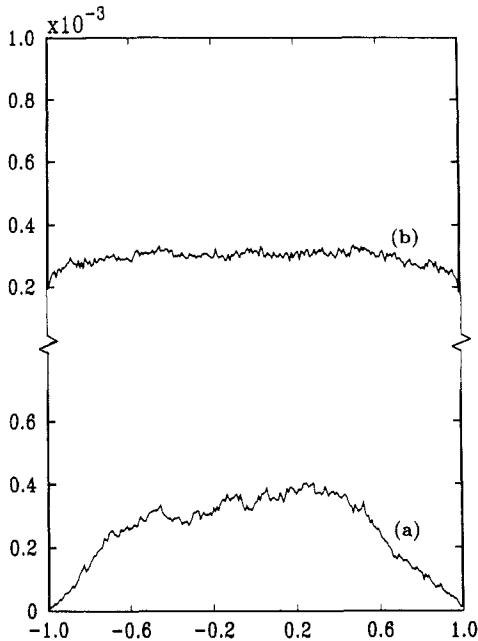


**Figure 6.** Simulation data for the probability distribution,  $P(x, t)$ , that the substrate is characterized by a density difference equal to  $x$  in the reaction-controlled limit. (a) Results from averaging of 1500 configurations of a one-dimensional substrate of linear dimension 250 for times  $16\,000 \leq t \leq 20\,000$ . (b) 15 000 configurations for a square of 256 sites with  $1000 \leq t \leq 1300$ .

## 6. Conclusions

We have investigated the kinetics of the monomer-monomer catalysis model in the mean-field limit. By modelling the substrate as a complete graph, one can describe the kinetics in terms of a one-dimensional stochastic process with hopping probabilities dependent on the density and the rates of adsorption and reaction. In the continuum limit, the probability distribution of surface coverage obeys a Fokker-Planck equation, with a state-dependent diffusion coefficient that reflects the composition dependence of the hopping probabilities. When the adsorption probabilities of  $A$  and  $B$  are unequal, the system saturates in a time of order unity, independent of lattice size. For equal adsorption probabilities of  $A$  and  $B$ , the average surface coverage is stationary,

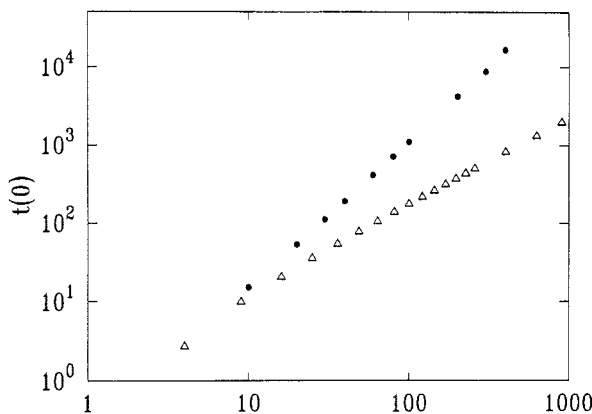


**Figure 7.** Dependence of the mean saturation time on the number of sites for a system initially containing a random distribution of 50% *A*s and 50% *B*s, in the reaction-controlled limit. ●, one dimension; and Δ, two dimensions.

corresponding to a reactive steady state within a rate equation approximation. However, diffusive fluctuations eventually drive a finite-sized system to saturation in a time proportional to the number of catalyst sites. Owing to the ‘stickiness’ of the stochastic process as saturation is approached, there is an anomalously large probability density for nearly full substrates at long times, compared with a constant diffusivity system. Monte-Carlo simulations of the monomer–monomer model show that basic dynamical features of the process agree with mean-field predictions for substrate dimensionality  $d \geq 2$ , but that substantial differences exist for  $d = 1$ . This suggests that the upper critical dimension of the substrate for the monomer–monomer process is  $d_c = 2$ .

The methodology outlined here can be usefully applied to a wider variety of catalytic processes. For example, if the physically-relevant possibility of desorption of reactants from the substrate occurs, in addition to desorption of the reaction product, then there are no true absorbing states. Therefore the system relaxes to a steady state which is determined by the competition between desorption, which tends to empty the substrate, and the catalytic reaction, which drives the system towards saturation. This competition underlies a bistability transition [17, 18], which can be understood at the mean-field level by the methods of this paper [18].

A second very interesting example is the monomer–dimer model [6, 7, 9, 10, 19–22], where one of the species adsorbs and dissociates, so that it occupies two adjacent lattice sites. This has been proposed as a model for the oxidation of carbon monoxide by oxygen on platinum, for example [6, 7]. Monte-Carlo simulations of the monomer–dimer process in the adsorption-controlled limit indicate that this system reaches a putative reactive steady state for a certain range of the relative deposition rates of *A* and *B* [6–9]. However, there is no true steady state in a finite-size system since the saturated catalyst is the only true absorbing state. From this viewpoint, a primary issue is to determine how long it takes before saturation is reached. Within the Fokker–Planck description, the monomer–dimer reaction induces a bias *away* from the true absorbing states, which leads to a saturation time that varies exponentially in the size of the system rather than linearly. Thus the master equation description demonstrates that the reactive steady-states predicted by the rate equation for the monomer–dimer and monomer–monomer processes are of completely different characters.



More interestingly, the master equation approach indicates that there is a fundamental difference between the adsorption-controlled and reaction-controlled limits for the monomer-dimer process. As a function of the surface reaction rate, there appears to be a transition from a regime where the saturation time grows as a power law in the system size to a regime where the saturation time grows exponentially in the size. This suggests a considerably richer phase diagram for the monomer-dimer process than has been appreciated thus far. These features will be treated in a future publication.

## Acknowledgments

We gratefully acknowledge grant #DAAL03-89-K-0025 from the Army Research Office for partial support of this research. Db-A thanks the Donors of the Petroleum Research Foundation for support and the warm hospitality of the Center for Polymer Studies at Boston University while carrying out part of this research.

## References

- [1] Campbell I M 1988 *Catalysis at Surfaces* (New York: Chapman and Hall)
- [2] Adamson A 1982 *Physical Chemistry of Surfaces* (New York: Wiley)
- [3] Williams E D, Thiel P A, Weinberg W H and Yates J T Jr 1980 *Aspects of the Kinetics and Dynamics of Surface Reactions* ed U Landman (New York: AIP) pp 275-83
- [4] Engl T and Ertl G 1979 *Advances in Catalysis* vol 28 (New York: Academic) p 1
- [5] Bernasek S L, Lenz K, Poelsema B and Comsa G 1987 *Surf. Sci.* **183** L319
- [6] Ziff R M, Gulari E and Barshad Y 1986 *Phys. Rev. Lett.* **56** 2553
- [7] Ziff R M and Fichthorn K 1986 *Phys. Rev. B* **34** 2038
- [8] Fichthorn K A, Ziff R M and Gulari E 1988 *Catalysis 1987* ed J W Ward (Amsterdam: Elsevier) p 883
- [9] Dickman R 1986 *Phys. Rev. A* **34** 4246
- [10] Meakin P and Scalapino D 1987 *J. Chem. Phys.* **87** 731
- [11] Dickman R and Burschka M A 1988 *Phys. Lett.* **127A** 133
- [12] ben-Avraham D, Redner S, Considine D and P Meakin 1990 *J. Phys. A: Math. Gen.* **23** L613
- [13] Karlin S and Taylor H M 1975 *A First Course in Stochastic Processes* (New York: Academic)
- [14] Abramowitz M and Stegun I A 1970 *Handbook of Mathematical Functions* (New York: Dover)
- [15] Wicke E, Kumman P, Keil W and Scheiffel J 1980 *Ber. Bunsenges. Phys. Chem.* **4** 315
- [16] Van Kampen N G 1981 *Stochastic Processes in Physics and Chemistry* (Amsterdam: North Holland)
- [17] Fichthorn K, Gulari E and Ziff R M 1989 *Phys. Rev. Lett.* **63** 1527
- [18] Considine D, Redner S and Takayasu H 1989 *Phys. Rev. Lett.* **63** 2857
- [19] Grinstein G, Lai Z-W and Browne D A 1989 *Phys. Rev. A* **40** 4820
- [20] Kaukonen H-P and Nieminen R M 1989 *J. Chem. Phys.* **91** 4380
- [21] Fischer P and Titulaer U M 1990 *Preprint*
- [22] Sadiq A 1987 *Z. Phys. B* **67** 211  
Yaldram K and Sadiq A 1989 *J. Phys. A: Math. Gen.* **22** L925